Gonio-spectral imaging of paper and cloth samples under oblique illumination conditions based on image fusion techniques

Yoshinori Akao[1, 3], Norimichi Tsumura[1], Patrick G. Herzog[2, 4], Yoichi Miyake[1] and Bernhard Hill[2]

[1]Graduate School of Science and Technology, Chiba University, Japan,

[2]Technical Electronics Institute, Aachen University of Technology, Aachen, Germany

[3]National Research Institute of Police Science, Japan

[4]Color AIXperts GmbH, Aachen, Germany

*A part of this work was presented at IS&T's PICS 2003 Conference.

Y. Akao, N. Tsumura, Y. Miyake, P. G. Herzog and B. Hill, Efficient gonio-spectral imaging for diffuse objects based on optical reflectance properties, *Proc. PICS 2003*, IS&T, Rochester, NY, 2003, pp.188-193.

Abstract

In this paper, we propose an effective method for gonio-spectral imaging of paper and cloth samples under oblique illumination conditions. High-resolution gonio-spectral images are synthesized from a basic spectral image and gonio-monochrome images. The method is based on gonio-spectral image fusion composed of two components, conventional spatial fusion and geometrical fusion. The proposed geometrical fusion synthesizes images at different geometries and is introduced by modeling the optical reflection properties with a dichromatic reflection model. The validity of this method is confirmed by gonio-spectral measurements of paper samples, and experiments are performed on Japanese washi paper and European cloth.

Keywords

spectral imaging, gonio-photometry, papers, cloths, oblique illumination, image fusion

Introduction

Paper and cloth are widely used as materials in the archiving of documents, pictures, art paints, historical clothes, and so on. Internet museums (E-museum) and Internet shopping (E-commerce) have been increasingly used in recent years due to the drastic improvement in information technology that enables the exchange of large amounts of image data through computer networks. However, in E-museums, for example, the color reproduction of paints is highly dependent on the spectral characteristics of the imaging devices and illumination used in recording the images. Furthermore, present image reproduction does not record the material characteristics of surfaces such as gloss, roughness, texture, scratch, defects, bumps, and dents.

In recent years, the multi-spectral imaging method[1-9] has been developed to record the precise color information of objects, independent from the spectral characteristics of the imaging devices and illumination. Furthermore, the gonio-photometric imaging method[10-13] was developed to record the spectral reflectance of 3-D objects, and it is effective in recording precise characteristics of materials.

In the case of paper and cloth, high spatial resolution imaging is required to capture the material characteristics, since the textures of these samples are very fine and contain high spatial frequency. However, this requires a large amount of data and much measurement and computing time. A number of data reduction techniques have been proposed, for example principal component analysis[14-18], Wiener estimation, and modeling of optical reflection properties. In a simpler approach proposed by Imai *et al.*[4], high-resolution spectral images are reproduced by the fusion of a high-resolution

monochrome image and a low-resolution spectral image.

For paper and cloth, oblique illumination is also important since the textures and characteristics of the sample surfaces are visualized with light-and-shade information. However, characteristics of paper and cloth cannot be recorded precisely at an oblique lighting geometry by spectral imaging with band-limited filters since the power of the reflected light is generally not strong in such geometries and it is influenced by the noise of the CCD.

In this paper, we introduce an effective method for gonio-spectral imaging of paper and cloth samples under oblique illumination geometries by synthesizing a high-resolution monochrome image and a low-resolution spectral image. The proposed method is based on two image fusions—spatial fusion, proposed by Imai *et al.*[4], and geometrical fusion, introduced in this paper. Geometrical fusion synthesizes images at different geometries, a spectral image at a geometry of 45/0 and gonio-monochrome images at geometries of 81/0 and 87/0. Conventional spatial fusion only takes images at one geometry. Since the images under oblique lighting conditions are only captured as monochrome images, the effect of noise is reduced compared to spectral imaging with band-limited filters. Our method is introduced by the simple modeling of optical reflection properties based on a dichromatic reflection model[19].

Methods

Shafer proposed the dichromatic reflection model[19] showing that the reflected light from inhomogeneous dielectric materials can be expressed by the linear combination of

two components, surface reflection and body reflection. The surface reflection is due to specular reflection from the surface of the sample, and is directed towards a mirror-wise reflection against the surface normal. The body reflection component is diffusely reflected in all directions, mainly due to surface roughness and multiple reflections by pigments such as colorants in the subsurface region. The spectral radiance $\mathbf{f}(\boldsymbol{r})$ at the image coordinate $\boldsymbol{r}$ at an illumination angle θ_i and observation angle θ_o is represented as,

$$\boldsymbol{f}(\boldsymbol{r},\theta_i,\theta_o) = \boldsymbol{f}_s(\boldsymbol{r},\theta_i,\theta_o) + \boldsymbol{f}_b(\boldsymbol{r},\theta_i,\theta_o)\,, \tag{1}$$

where the subscripts s and b show the specular and body reflection components respectively. The spectral radiance is expressed using discrete vector notation, where the spectral radiances at n different wavelengths in the visible wavelength region are represented as $\boldsymbol{f}(\boldsymbol{r},\boldsymbol{\theta}) = [f_1(\boldsymbol{r},\boldsymbol{\theta}), f_2(\boldsymbol{r},\boldsymbol{\theta}), \cdots f_n(\boldsymbol{r},\boldsymbol{\theta})]^T$, where the vector $\boldsymbol{\theta}$ is a geometrical parameter representing the illumination and observation direction, i.e. combining θ_i and θ_o. In Equation (1), the geometrical and spectral components can be represented separately as,

$$\boldsymbol{f}(\boldsymbol{r},\boldsymbol{\theta}) = k_s(\boldsymbol{r},\boldsymbol{\theta})\boldsymbol{e}_s(\boldsymbol{r}) + k_b(\boldsymbol{r},\boldsymbol{\theta})\boldsymbol{e}_b(\boldsymbol{r})\,, \tag{2}$$

where $\boldsymbol{e}_s$ and $\boldsymbol{e}_b$ are unit vectors of the spectral component and k_s and k_b are the intensities of the reflected light dependent on the geometrical conditions.

In this paper, we assume that the dichromatic reflection model is valid for paper and cloth. We also assume the diffuse reflection component is dominant, i.e. $k_b >> k_s$, in our imaging system. This is because samples are illuminated obliquely and observed from their normal direction, i.e. the observation direction is far from the specular

direction. In this case, Eq. (2) can be normalized by the radiance at geometry $\boldsymbol{\theta}_0$ as,

$$\boldsymbol{f}(\boldsymbol{r},\boldsymbol{\theta}) = k(\boldsymbol{r},\boldsymbol{\theta})\,\boldsymbol{f}(\boldsymbol{r},\boldsymbol{\theta}_0)\ , \tag{3}$$

where $\boldsymbol{f}(\boldsymbol{r},\boldsymbol{\theta}_0)$ is the spectral radiance at the basic geometry $\boldsymbol{\theta}_0$, and $k(\boldsymbol{r},\boldsymbol{\theta})$ is the normalized coefficient for the gonio property,

$$k(\boldsymbol{r},\boldsymbol{\theta}) = \frac{\|f(\boldsymbol{r},\boldsymbol{\theta})\|}{\|f(\boldsymbol{r},\boldsymbol{\theta}_0)\|}\ . \tag{4}$$

If the spectral radiance $\boldsymbol{f}(\boldsymbol{r},\boldsymbol{\theta})$ is observed by a monochrome camera system with spectral sensitivity $\boldsymbol{s}$, the sensor value $g(\boldsymbol{r},\boldsymbol{\theta})$ can be written as,

$$g(\boldsymbol{r},\boldsymbol{\theta}) = \boldsymbol{s}\,\boldsymbol{f}(\boldsymbol{r},\boldsymbol{\theta})\ . \tag{5}$$

The monochrome image $g(\boldsymbol{r},\boldsymbol{\theta}_0)$ at the basic geometry $\boldsymbol{\theta}_0$ is calculated from the basic spectral image $\boldsymbol{f}(\boldsymbol{r},\boldsymbol{\theta}_0)$ using the factor $\boldsymbol{s}$. In the following, we can show from Eq. (3) and Eq.(5) that the ratio between $g(\boldsymbol{r},\boldsymbol{\theta})$ and $g(\boldsymbol{r},\boldsymbol{\theta}_0)$ gives $k(\boldsymbol{r},\boldsymbol{\theta})$. Then $k(\boldsymbol{r},\boldsymbol{\theta})$ is calculated from the basic spectral radiance and the monochrome sensor value by

$$\begin{aligned} k(\boldsymbol{r},\boldsymbol{\theta}) &= \frac{g(\boldsymbol{r},\boldsymbol{\theta})}{g(\boldsymbol{r},\boldsymbol{\theta}_0)} \\ &= \frac{g(\boldsymbol{r},\boldsymbol{\theta})}{\boldsymbol{s}\,\boldsymbol{f}(\boldsymbol{r},\boldsymbol{\theta}_0)}. \end{aligned} \tag{6}$$

Equations (3) and (6) demonstrate the principle of geometrical image fusion where the gonio-spectral image $\boldsymbol{f}(\boldsymbol{r},\boldsymbol{\theta})$ is represented by both the basic spectral image $\boldsymbol{f}(\boldsymbol{r},\boldsymbol{\theta}_0)$ and the gonio-monochrome images $g(\boldsymbol{r},\boldsymbol{\theta})$.

Figure 1 shows a flowchart of the proposed method. The basic spectral image $\boldsymbol{f}(\boldsymbol{r},\boldsymbol{\theta}_0)$ was obtained at a geometry of 45/0, and the gonio-monochrome images were obtained at various geometries where the illuminant direction was varied and the observation direction was fixed at normal to the sample. The ratio between the

gonio-monochrome images $g(\boldsymbol{r},\boldsymbol{\theta})$ and $g(\boldsymbol{r},\boldsymbol{\theta}_0)$ was obtained to give the coefficient for the gonio property $k(\boldsymbol{r},\boldsymbol{\theta})$. Here, $g(\boldsymbol{r},\boldsymbol{\theta}_0)$ is the basic monochrome image calculated from the basic spectral image.

In the next step, the power of the basic spectral image needs to be modulated by the coefficient $k(\boldsymbol{r},\boldsymbol{\theta})$ to synthesize a gonio-spectral image at geometry $\boldsymbol{\theta}$. This process is called geometrical image fusion. For simplicity, the calculation was performed in XYZ color space. The basic spectral image was transformed to the XYZ tristimulus value vector $\boldsymbol{x}_1$ under the illuminant for reproduction, thereafter $\boldsymbol{x}_1$ was multiplied by the coefficient $k(\boldsymbol{r},\boldsymbol{\theta})$ to obtain the tristimulus value vector $\boldsymbol{x}_2$ at geometry $\boldsymbol{\theta}$. In this process, spatial image fusion was also performed. The spatial resolution of the basic tristimulus image $\boldsymbol{x}_1$ was matched with that of the high-resolution gonio-monochrome images using the nearest-neighbor method. Then the tristimulus value $\boldsymbol{x}_2$ was displayed on the monitor according to the profile of the monitor.

Experiments

Gonio-spectral reflection property of paper sample

Spatially averaged gonio-spectral reflection properties from 390 nm to 730 nm of Japanese washi paper (Okamura Takao Paper Mill, "Ranka") of size 60 mm by 150 mm, were measured by a gonio spectrophotometer (Murakami Color Research Laboratory, GCMS-4) at 72 different incident angles from 9° to 80° where the observation angle was fixed at 0° from the surface normal.

Figure 2 (a) shows the result of the gonio-spectral reflectance property measurements

of the paper. The horizontal axes show the wavelength and incident angle, and the vertical axis shows the relative radiance factor. The relative radiance factor is normalized by the spectral radiance from the reference diffuse white plate in the gonio spectrophotometer. Figure 2 (b) shows the relative radiance factor at geometry 45/0, and Fig. 2 (c) shows the correlation coefficient between geometry 45/0 and other geometries. The calculation of the correlation coefficient was based on Pearson's product-moment correlation coefficient,

$$R(\boldsymbol{\theta},\boldsymbol{\theta}_0)=\frac{\left\langle\left(o(\boldsymbol{\theta},\lambda_i)-\langle o(\boldsymbol{\theta},\lambda_i)\rangle\right)\left(o(\boldsymbol{\theta}_0,\lambda_i)-\langle o(\boldsymbol{\theta}_0,\lambda_i)\rangle\right)\right\rangle}{\sqrt{\left\langle\left(o(\boldsymbol{\theta},\lambda_i)-\langle o(\boldsymbol{\theta},\lambda_i)\rangle\right)^2\right\rangle}\sqrt{\left\langle\left(o(\boldsymbol{\theta}_0,\lambda_i)-\langle o(\boldsymbol{\theta}_0,\lambda_i)\rangle\right)^2\right\rangle}}, \tag{8}$$

where $o(\boldsymbol{\theta},\lambda_i)$ is the reflectance of the wavelength λ_i at geometry $\boldsymbol{\theta}$. The vector $\boldsymbol{\theta}_0$ is the geometry of the basic spectral imaging, 45/0. The brackets $\langle\ \rangle$ represent statistical averaging at wavelength λ_i. Strong correlation was obtained between geometry 45/0 and other geometries, which showed that the relative spectral distribution hardly changes with measurement geometry. Therefore the model used for gonio-spectral reflection properties was maintained at a spatially macroscopic scale. Figure 2 (d) shows the coefficient for the gonio property calculated with Eq. (3).

The gonio-spectral reflectance of a paper sample was examined also at a spatially fine scale, i.e. an analysis was performed at each pixel of a textured image consisting of light-and-shade induced by roughness, bumps, and dents of the sample surface. The sample for analysis was Japanese washi paper (Yamada Shokai, "Nunomeshi"). Patterns of bumps and dents like ripple marks were formed on the surface, and it felt like hard

cloth. The spectral distribution at each point of the texture was obtained using a spectral imaging system[19] (Applied Spectral Imaging, SD-200). The geometry of measurement was 45/0, and the wavelength ranged from 390 nm to 730 nm. The resolution of the measured spectrum was dependent on the wavelength, since the system was based on Fourier-transform spectroscopy; the resolution was 1 nm at 400 nm, and 4 nm at 700 nm. The size of the region of interest was 7.4 mm by 7.1 mm, and the number of pixels was 48 by 46, which corresponds to sampling at 160 ppi.

Figure 3(a) shows a monochrome image of the washi paper sample. Figure 3(b) shows the averaged spectral radiance in the texture and Fig. 3(c) shows the correlation coefficient map of the spectrum at each pixel. The correlation coefficient was calculated from the averaged spectrum and the spectral reflectance at each pixel based on Pearson's product-moment correlation coefficient, as shown by Eq. (7). The correlation coefficient was nearly 1.0 at most parts of the sample, however there were some areas with extremely low correlation. Comparing Fig. 3(a) and Fig. 3(c) it can be seen that the areas of low correlation correspond to specular parts. The proposed model for gonio-spectral reflection properties was approximately maintained at a spatially fine scale except for the specular parts.

Gonio-spectral image fusion

Spectral images were obtained from a multispectral camera (RWTH-Aachen, ITE)[9]. This device acquires multi band images by irradiating light of limited wavelength range onto samples, and is classified as an active type system. In front of a light source, sixteen kinds of bandpass interference filters were placed with central wavelengths 400

nm, 420nm, … , 700 nm and FWHM bandwidth 20 nm. Reflected light from the sample was imaged by a 12-bit monochrome chilled CCD camera (Photometrics, CH250H). Binning of the CCD was set to 3 by 3 pixels, and the number of pixels was 677 by 677. The sixteen multispectral values were converted into 61 spectral values of 5 nm intervals from 400 nm to 700 nm by a special transformation matrix. The average color difference of 24 color patches (Macbeth Color Checker) was 1.2 in the CIE E94 unit. Gonio monochrome images were also taken by the CCD camera of the multispectral camera. In this case, binning of the CCD camera was not set, and the number of pixels was 2031 by 2031. The light source for monochrome imaging was a halogen lamp (Phillips, 12 V, 50 W). An infrared cut filter was used and light of wavelength longer than the upper limit wavelength of the multispectral camera was almost eliminated. There was no problem of image registration between the spectral image and the monochrome image since these two images were obtained with the same CCD camera.

With this system, gonio-spectral images of Japanese washi paper (Okamura Takao Paper Mill, "Ranka") and a piece of cloth (Flechtatelier, “Linea”, 61% cotton, 30% viscose, 9% polyester) were taken. A basic spectral image was obtained at geometry 45/0, and gonio monochrome images were taken at geometries 81/0 and 87/0. Extreme oblique illumination was used for visualizing roughness, texture, and bumps and dents of the sample surfaces. From the basic spectral image and monochrome images at geometries 81/0 and 87/0, spectral images were generated at geometries 81/0 and 87/0. The obtained spectral reflectance reproduced color images under illuminant A and D65.

Figure 4 shows results for the Japanese washi paper. Figure 4 (a) shows color

images of Japanese washi paper reproduced under illuminant D65 at geometry 45/0. The color of the samples was measured precisely with this system. Figure 4 (b) shows the reproduced image at geometry 81/0, and Fig. 4 (c) shows that at geometry 87/0. Texture of light-and-shade induced by non-uniformity of fibers on the paper surface was represented sharply and wiping marks formed in the process of drying the paper were also represented. Such texture was not perceived at geometry 45/0. The appearance of the texture was differently reproduced at geometries 81/0 and 87/0.

Figure 5 shows the result for the cloth sample. Figure 5 (a) shows the color image from low-resolution spectral raw data at geometry 45/0 reproduced under illuminant D65. Figure 5 (b) shows the image reproduced at geometry 81/0 and illuminant A, and Fig. 5 (c) shows that at geometry 87/0 and illuminant D65. Surface roughness of the cloth was expressed well. Differences between materials and soft and hard parts could be also perceived from the differences of the gonio reflection properties. Surface texture induced by the thread of the cloth was recorded precisely.

Figure 6 shows the effects of the image fusion technique. These figures are a part of the cloth sample. As shown in Fig. 6 (a), the basic spectral image was not sharp and the resolution was not sufficient to image the fine texture of the sample because only 3 by 3 CCD binning was applied. On the contrary, the monochrome image in Fig. 6 (b) has three times higher resolution and represents light and shade induced by oblique illumination very well, as well as the fine textures of the fibers. The spectral image shown in Fig. 6 (c) was synthesized from Fig. 6 (a) and Fig. 6 (b). Precise texture information is displayed together with accurate color information based on the spectral

data. Therefore the gonio reflection properties, including the appearance of surface texture, were precisely represented in the reproduced images. The material characteristics of the experimental samples were faithfully recorded and represented by a smaller number of sampling points than in the previous method.

Discussion

In this study, gonio-spectral image fusion was proposed and experiments were performed with paper and cloth samples under oblique illumination conditions. The texture was recorded faithfully at a spatially high-resolution to provide the material properties of these samples. The images were displayed with accurate color information based on spectral data. The effect of noise due to low light intensity was reduced by geometrical image fusion since the images under oblique illumination conditions were only captured as monochrome images without narrow band color filters. The method is also effective for data and measurement time reduction since the time-consuming spectral imaging of large amounts of data was performed only once, at geometry 45/0. The spatial resolution was enhanced by a spatial fusion technique, which is an advantage since the chromatic channels have a much lower spatial resolution than the luminance channel in human eyes.

The validity of the proposed method was proven at a spatially macroscopic scale, however it was not maintained to the same quality at specular parts of the samples as it is observed at a spatially fine scale. This is contrary to our initial assumption that specular reflected light could be ignored since the observation direction in this study

was far from the specular direction. In the synthesized images, specular reflection components might be detected even at oblique illumination conditions since the local surface normal of a rough surface has various directions. At the spatially macroscopic scale, specular components can be ignored since they are small and their spatial structure is fine. In high-resolution images, however, these specular components should not to be ignored when observing texture. In future studies, we will consider specular and diffuse components obtained separately by using polarized light [21] and then synthesized by a dichromatic reflection model for the faithful reproduction of material properties.

Conclusion

In this paper, we have proposed an effective method for gonio-spectral imaging of paper and cloth samples under oblique illumination conditions. High-resolution gonio-spectral images were synthesized by an image fusion technique. Geometrical image fusion was proposed to synthesize images of different geometries by modeling the optical reflection properties with a dichromatic reflection model. The validity of the technique was confirmed by gonio-spectral measurements of paper samples. Experiments were performed on Japanese washi paper and European cloth. The material characteristics were faithfully recorded and the appearance was precisely represented with a smaller number of sampling points than the previous method. The effects of specular reflection should be considered in future work.

References

1. P. D. Burns and R. S. Berns, Analysis of multispectral image capture, *Proc. of IS&T/SID's 4th color Imaging Conference*, Scottsdale, AZ, 1996, pp. 19-22 .
2. D. Saunders and J. Cupitt, Image processing at the national gallery: The VASARI project, *Natl. Gallery Tech. Bull.* **14**, 72-85 (1993).
3. H. Maitre, F. Schmitt, J. Crettez, Y. Wu and Y. Hardberg, Spectrophotometric image analysis of fine art paintings, *Proc. of IS&T/SID's 4th Color Imaging Conference,* Scottsdale, AZ, 1996, pp.50-53.
4. F. H. Imai and R. S. Berns, High-Resolution Multi-Spectral Image Archives: A Hybrid Approach, *Proc. of IS&T/SID's 6th Color Imaging Conference,* Scottsdale, AZ, 1998, pp. 224-227.
5. M. Yamaguchi, T. Teraji, K. Ohsawa, T. Uchiyama, H. Motomura, Y. Murakami and N. Ohyama, Image reproduction based on multispectral and multiprimary imaging: experimental evaluation, *Proc. of SPIE* **4663**: 15-26 (2002).
6. M. Hauta-Kasari, K. Miyazawa, S. Toyooka and J. Parkkinen, Spectral vision system for measuring color images, *J. Opt. Soc. Am. A* **16**, 2352-2362 (1999).
7. S. Tominaga, Multichannel vision system for estimating surface and illumination functions, *J. Opt. Soc. Am. A* **13**, 2163-2173 (1996).
8. H. Sugiura, T. Kuno, N. Watanabe, N. Matoba, J. Hayashi and Y Miyake, Development of a multispectral camera system, *Proc. SPIE* **3965**: 331-339 (2000).
9. B. Hill, F. W. Vorhagen, Multispectral Image Pick-up System, *U.S.Pat. 5,319,472*, Germany (1991).

10. H. Haneishi, T. Iwanami, T. Honma, N. Tsumura and Y. Miyake, Goniospectral imaging of three-dimensional objects, *J. Imaging Sci. Technol.* **45**, 451-483 (2001).
11. M. Tsuchida, Y. Murakami, T. Obi, M. Yamaguchi and N. Ohyama, High fidelity image reproduction using angular distribution of reflected spectral intensity, *Opt. Rev.* **8**, 444-450 (2001).
12. S. Tominaga, T. Matsumoto and N. Tanaka, 3D recording and rendering of art paintings, *Proc. of IS&T/SID's 9th Color Imaging Conference,* Scottsdale, AZ, 2001, pp. 337-341.
13. K. Tonsho, Y. Akao, N. Tsumura, Y. Miyake, Development of goniophotometric imaging system for recording reflectance spectra of 3D objects, *Proc. SPIE* **4663**: 370-378 (2002).
14. T. Jaaskelainen, J. Parkkinen and S. Toyooka, Vector-subspace model for color representation, *J. Opt. Soc. Am. A* **7**, 725-730 (1990).
15. D. H. Marimont, and B. A. Wandell, Linear model of surface and illuminant spectra, *J. Opt. Soc. Am. A* **9**, 1905-1913 (1990).
16. H. J. Trussell, Applications of Set Theoretic Methods to Color Systems, *Color Res. Appl.* **16**, 31-41 (1991).
17. Th. Keusen, Multispectral color system with an encoding format compatible with the conventional tristimulus model, *J. Imaging Sci. Technol.* **40**: 510-515 (1996).
18. F. König and W. Praefcke, Multispectral image encoding, *Proc. IEEE's Intern. Conf. on Image Proc. ICIP, Kobe, Japan,* 1999, **3**, pp.123-126.
19. S. A. Shafer, Using color to separate reflection components, *Color Research and*

Application, **10**: 210-218 (1985).

20. D. Cabib, R. A. Buckwald, Y. Garini and D. G. Soenksen, Spatially resolved Fourier transform spectroscopy (spectral imaging): a powerful tool for quantitative analytical microscopy, *Proc. of SPIE* **2678**: 278-291 (1996).
21. N. Ojima, H. Haneishi and Y. Miyake, The appearance of skin with make-up (II) (Analysis on surface topography of skin with make-up), Journal of the Society of Photographic Science and Technology of Japan, **56**, 264-269 (1993) [in Japanese].

Figure captions

Figure 1. Flowchart of gonio-spectral image fusion.

Figure 2 Gonio-spectral reflection properties of Japanese washi paper at a spatially macroscopic scale: (a) gonio-spectral reflection property, (b) spectral radiance factor at geometry 45/0, (c) correlation coefficient between geometry 45/0 and other geometries, and (d) coefficient for gonio property.

Figure 3. Spectral reflection properties of light-and-shade texture at a spatially fine scale: (a) monochrome image of the texture, (b) averaged spectral radiance of the texture, and (c) correlation coefficient map at each pixel.

Figure 4. Color images of the Japanese washi paper reproduced under illuminant D65, (a) from the basic spectral data at geometry 45/0, (b) from the synthesized spectral data at geometry 81/0, and (c) at geometry 87/0.

Figure 5. Reproduced color images of the European cloth sample, (a) from the basic spectral data at geometry 45/0 under illuminant D65, (b) from the synthesized spectral data at geometry 81/0 under illuminant A, and (c) at geometry 87/0 under illuminant D65.

Figure 6. Effects of gonio-spectral image fusion, (a) the basic spectral image, and (b)

high-resolution monochrome image at geometry 81/0 under illuminant D65, and (c) synthesis of the basic spectral image and oblique monochrome image.

Illustrations

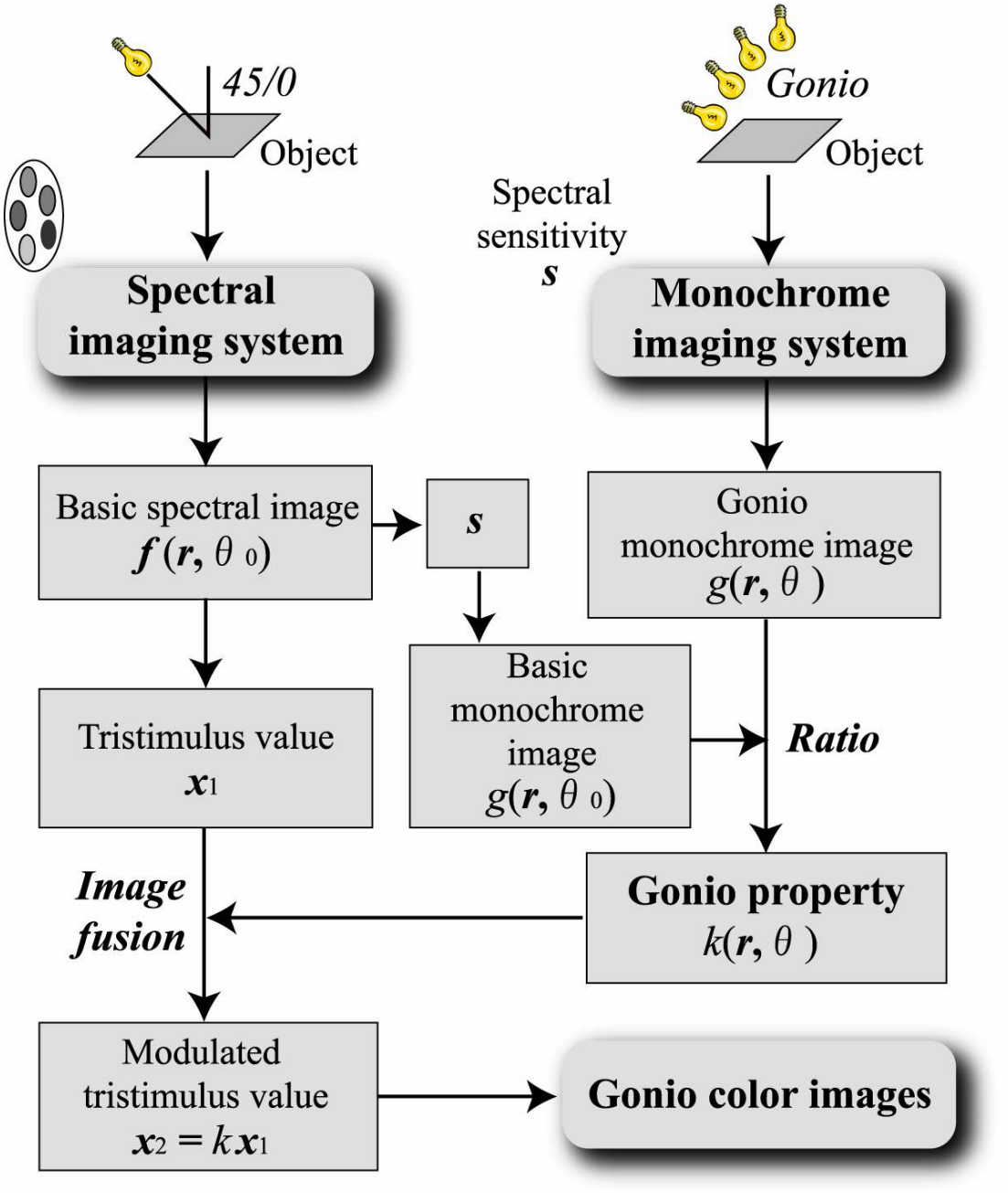

Figure 1

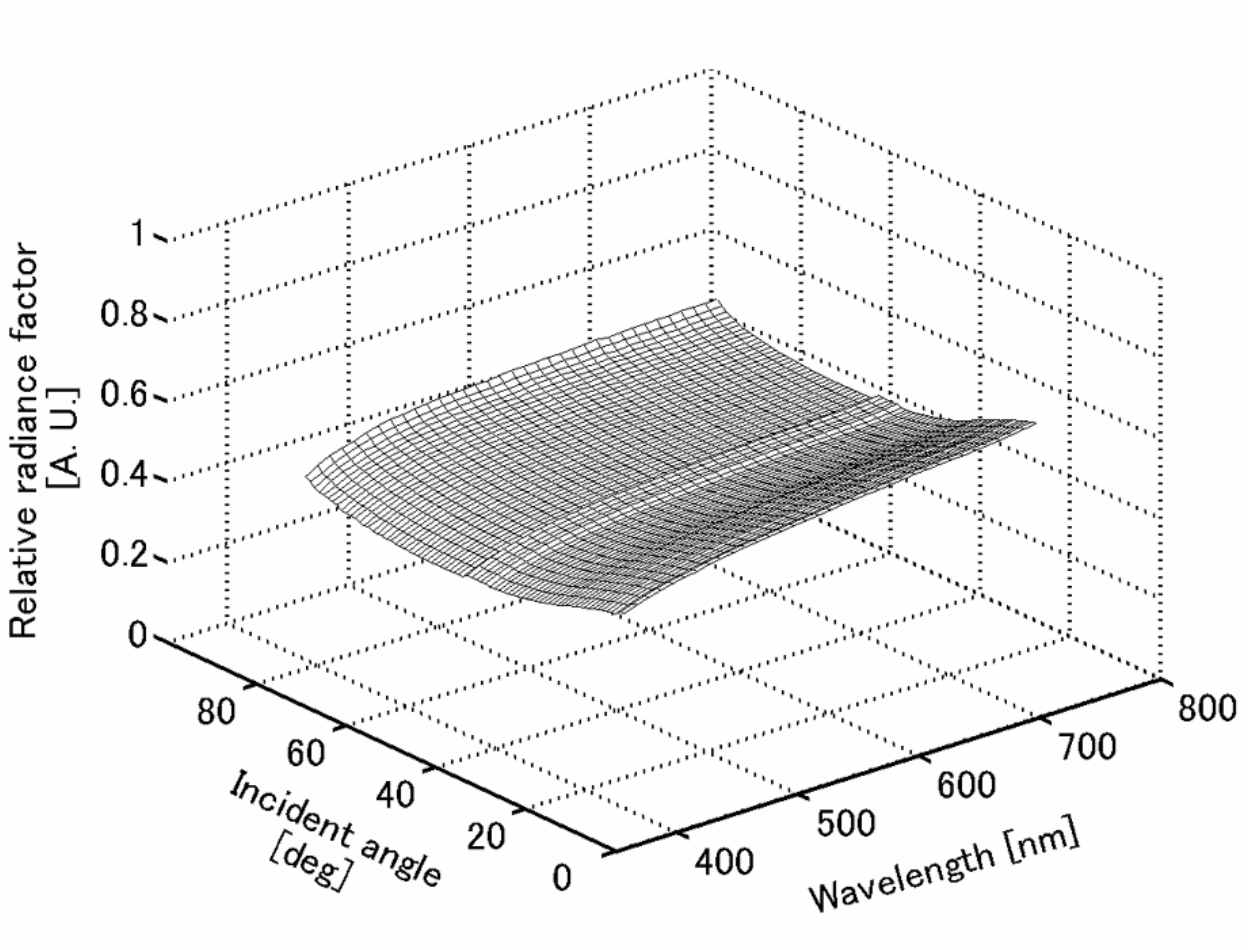
Relative radiance factor
[A. U.]
1
0.8
0.6
0.4
0.2
0
80
60
40
20
0
Incident angle
[deg]
400
500
600
700
800
Wavelength [nm]

Figure 2 (a)

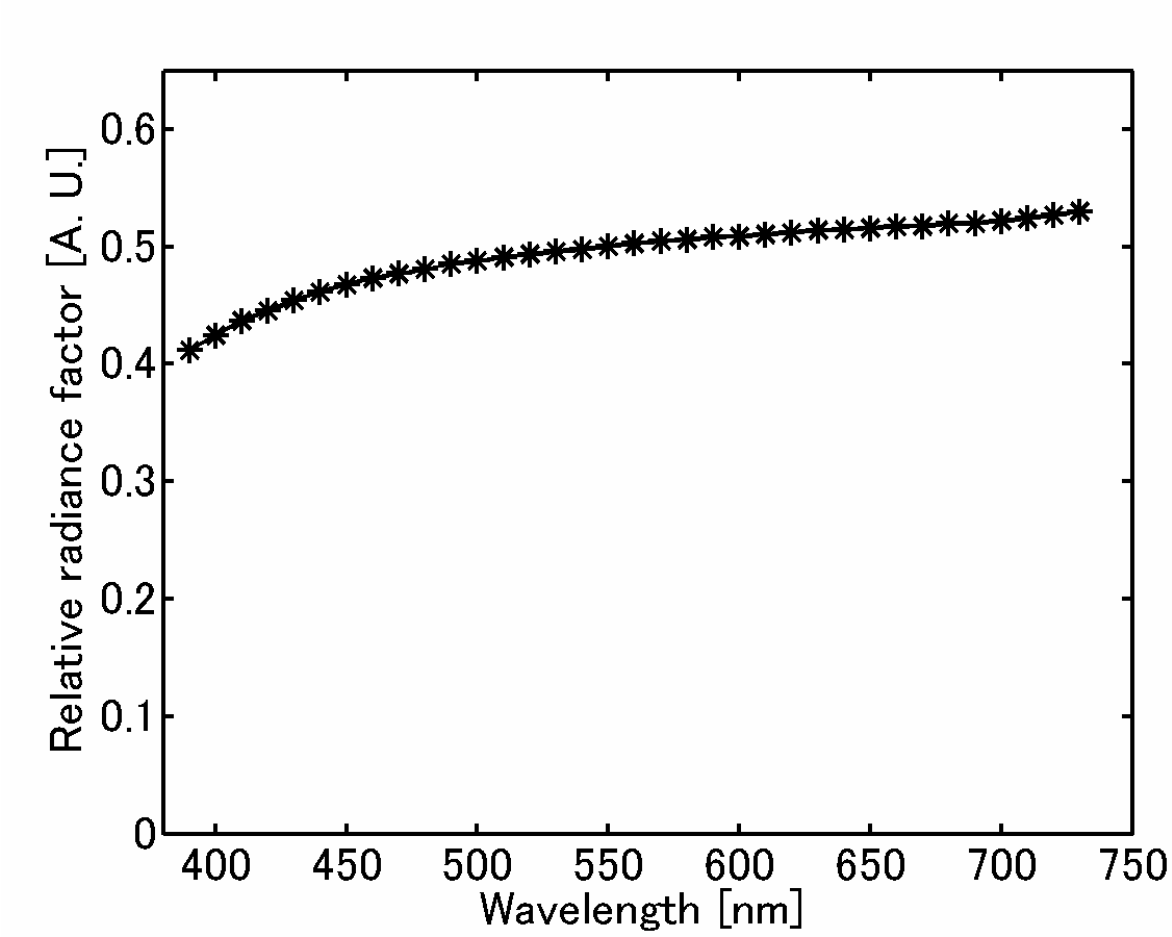
Relative radiance factor [A. U.]
0
0.1
0.2
0.3
0.4
0.5
0.6
400
450
500
550
600
650
700
750
Wavelength [nm]

Figure 2 (b)

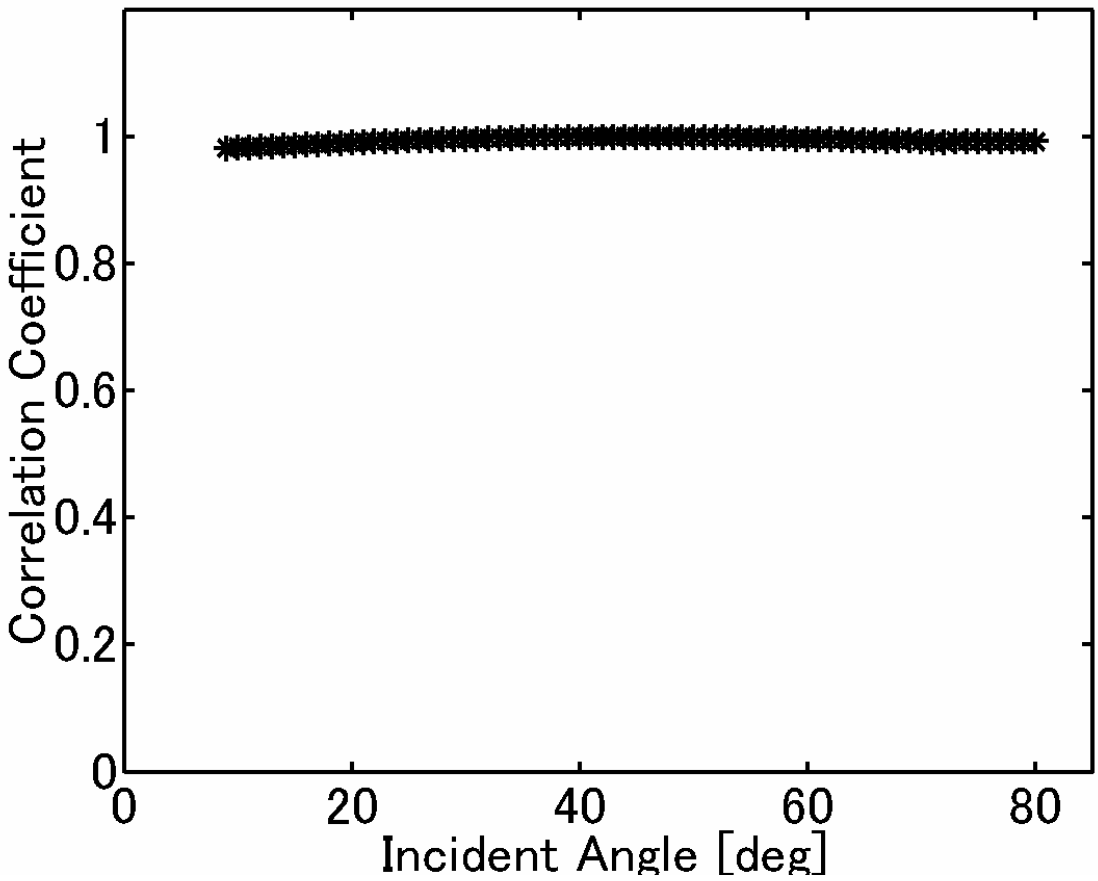
Correlation Coefficient
1
0.8
0.6
0.4
0.2
0
0
20
40
60
80
Incident Angle [deg]

Figure 2 (c)

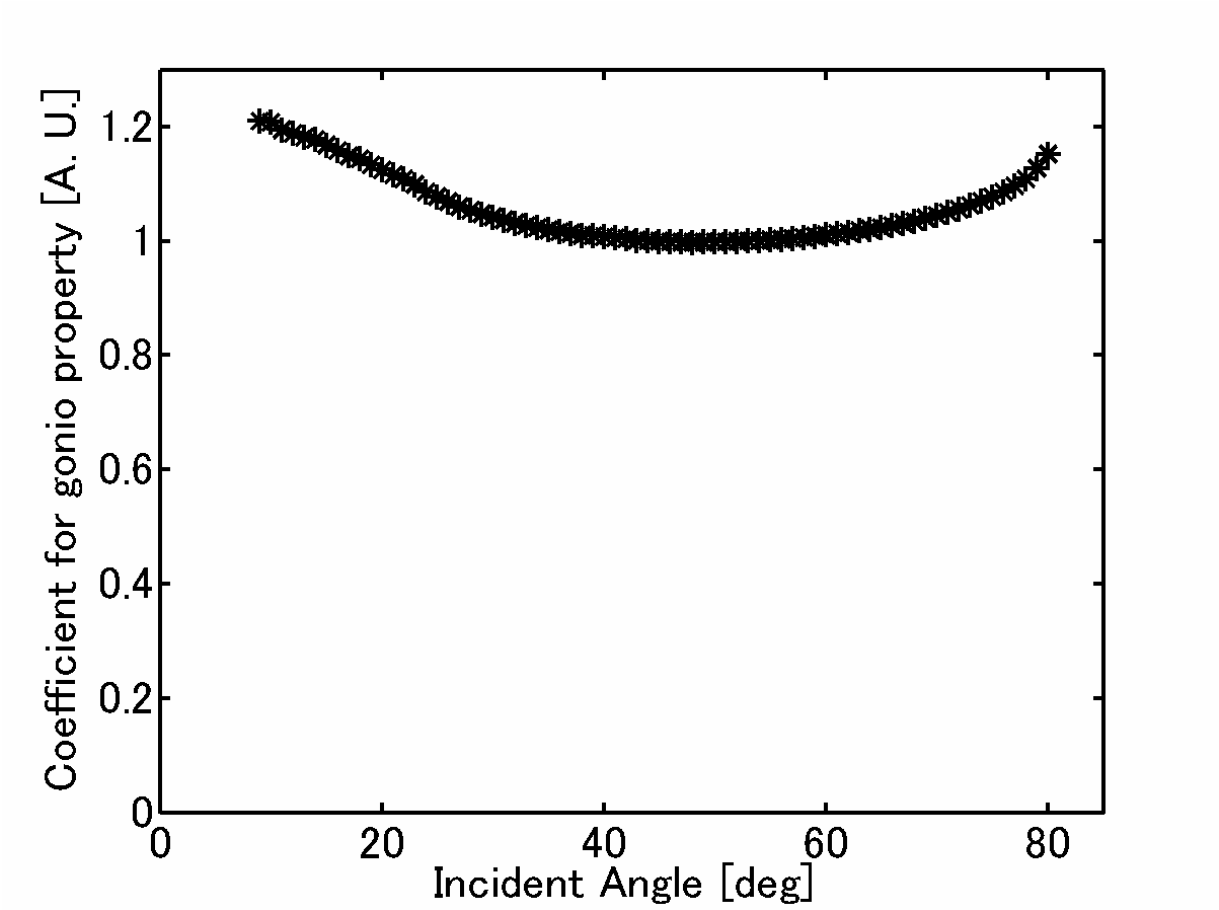
Coefficient for gonio property [A. U.]
1.2
1
0.8
0.6
0.4
0.2
0
0
20
40
60
80
Incident Angle [deg]

Figure 2 (d)

Figure 3 (a)

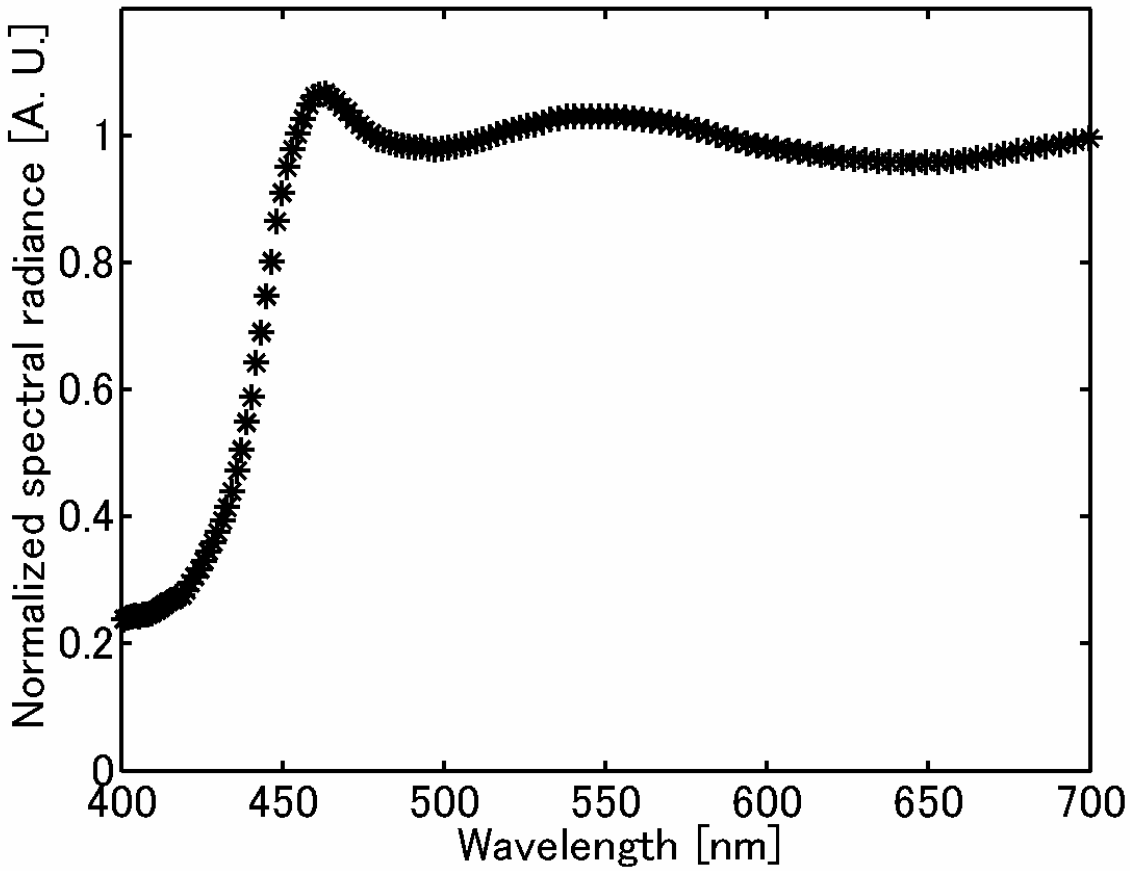
Normalized spectral radiance [A. U.]
0
0.2
0.4
0.6
0.8
1
400
450
500
550
600
650
700
Wavelength [nm]

Figure 3 (b)

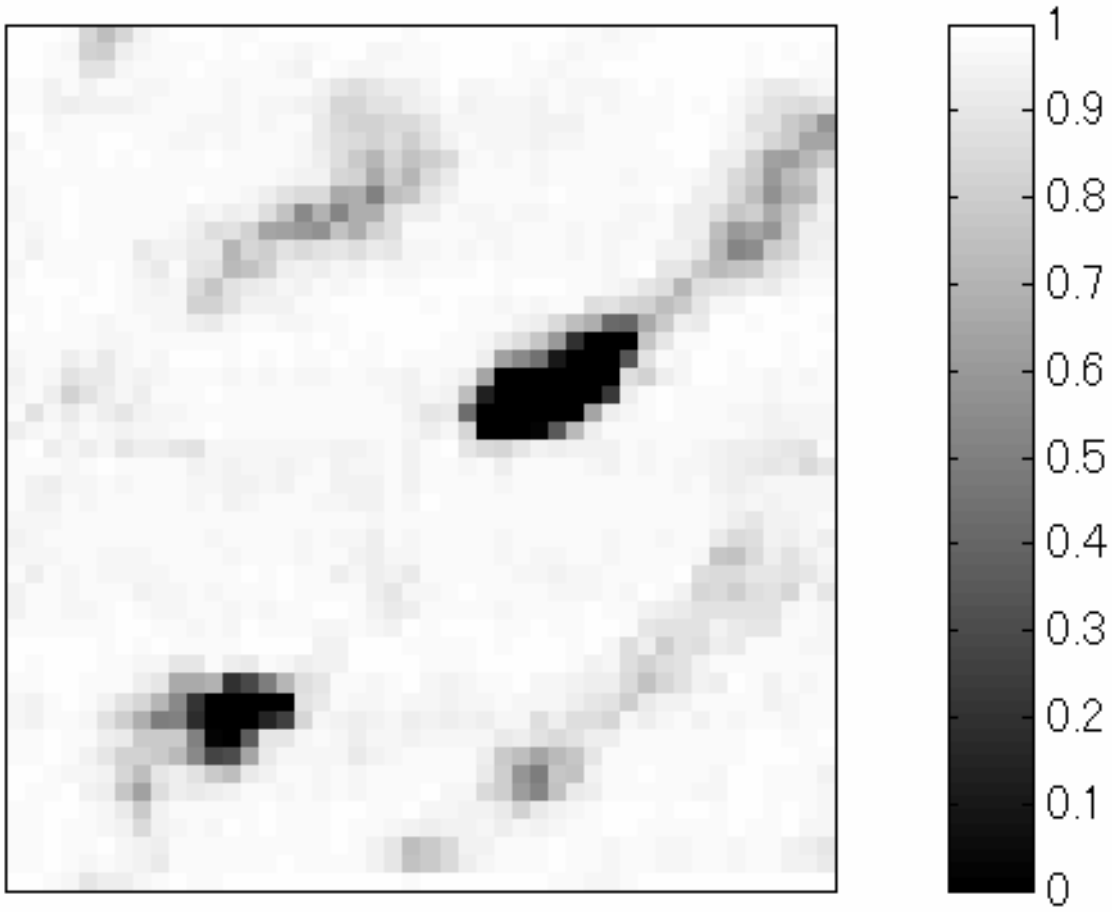

Figure 3 (c)

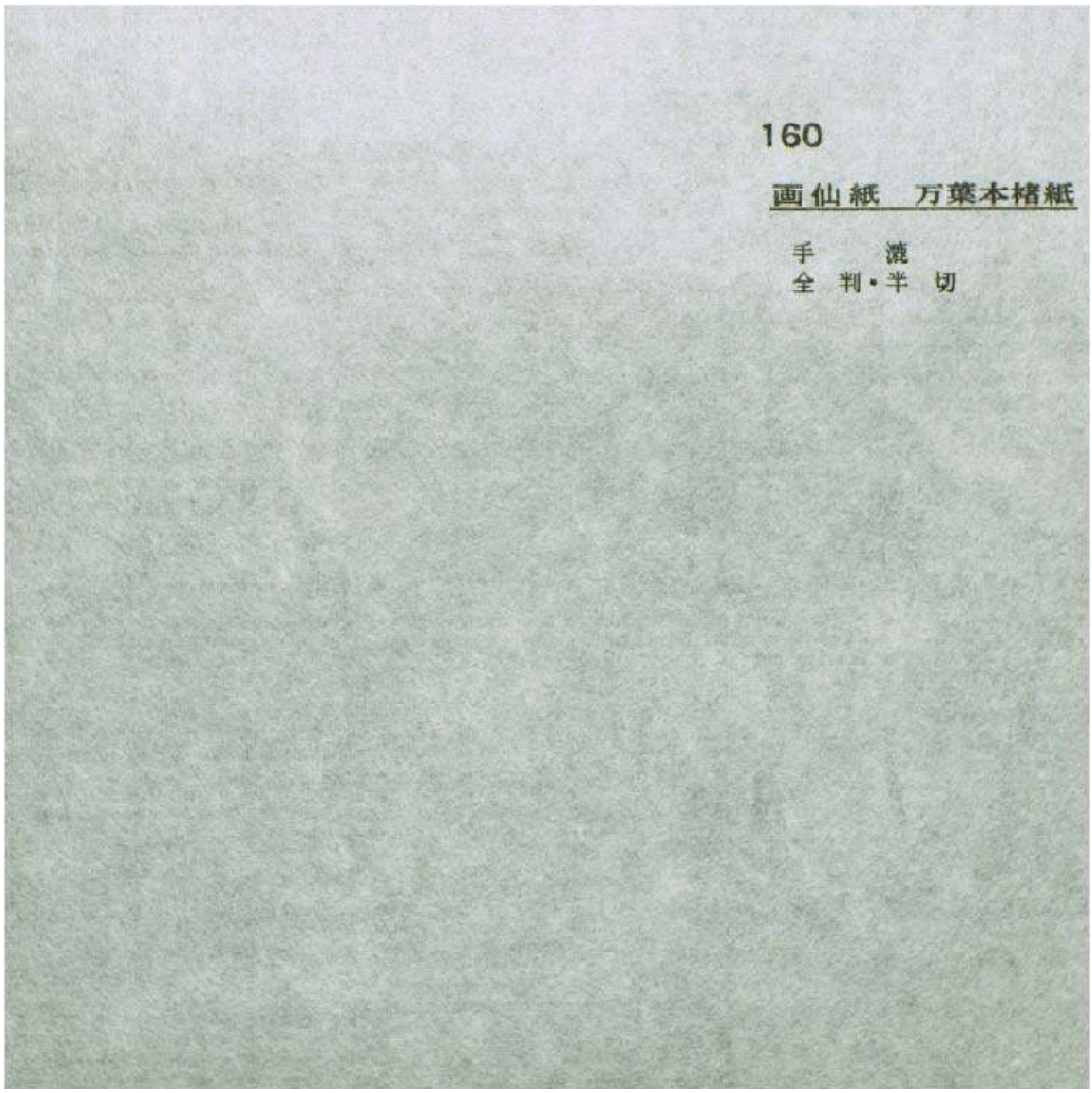

Figure 4 (a)

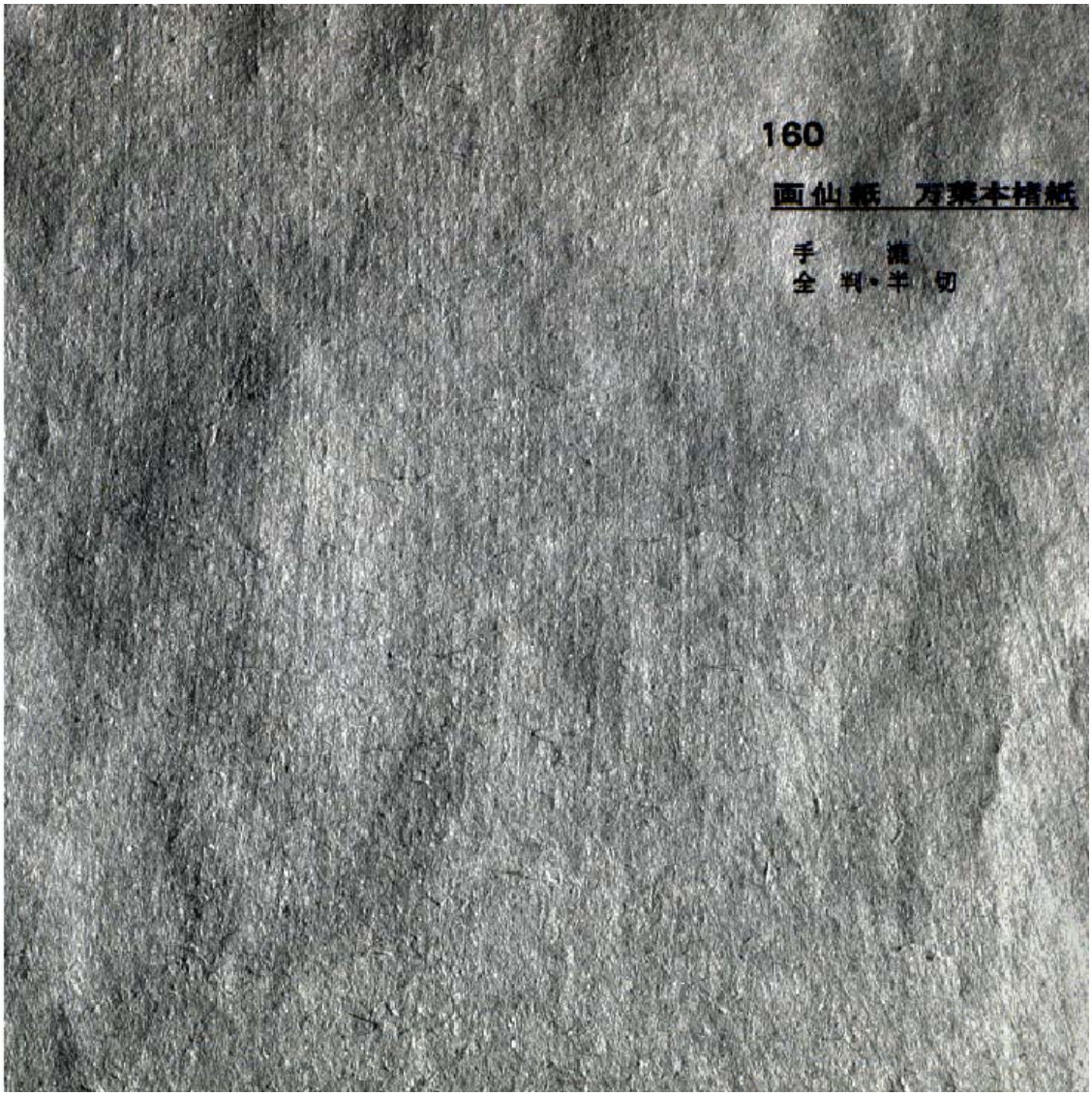

Figure 4 (b)

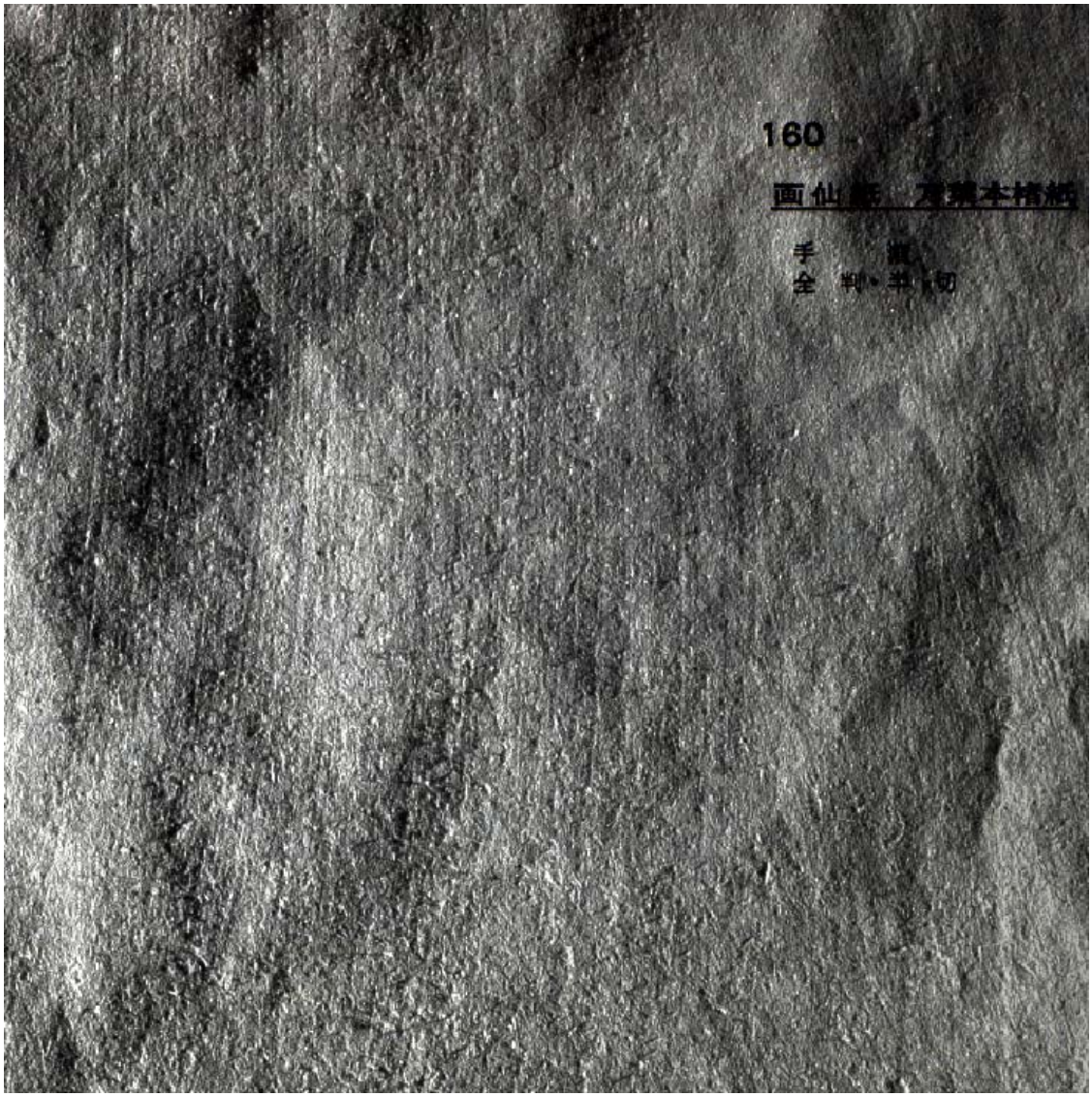

Figure 4 (c)

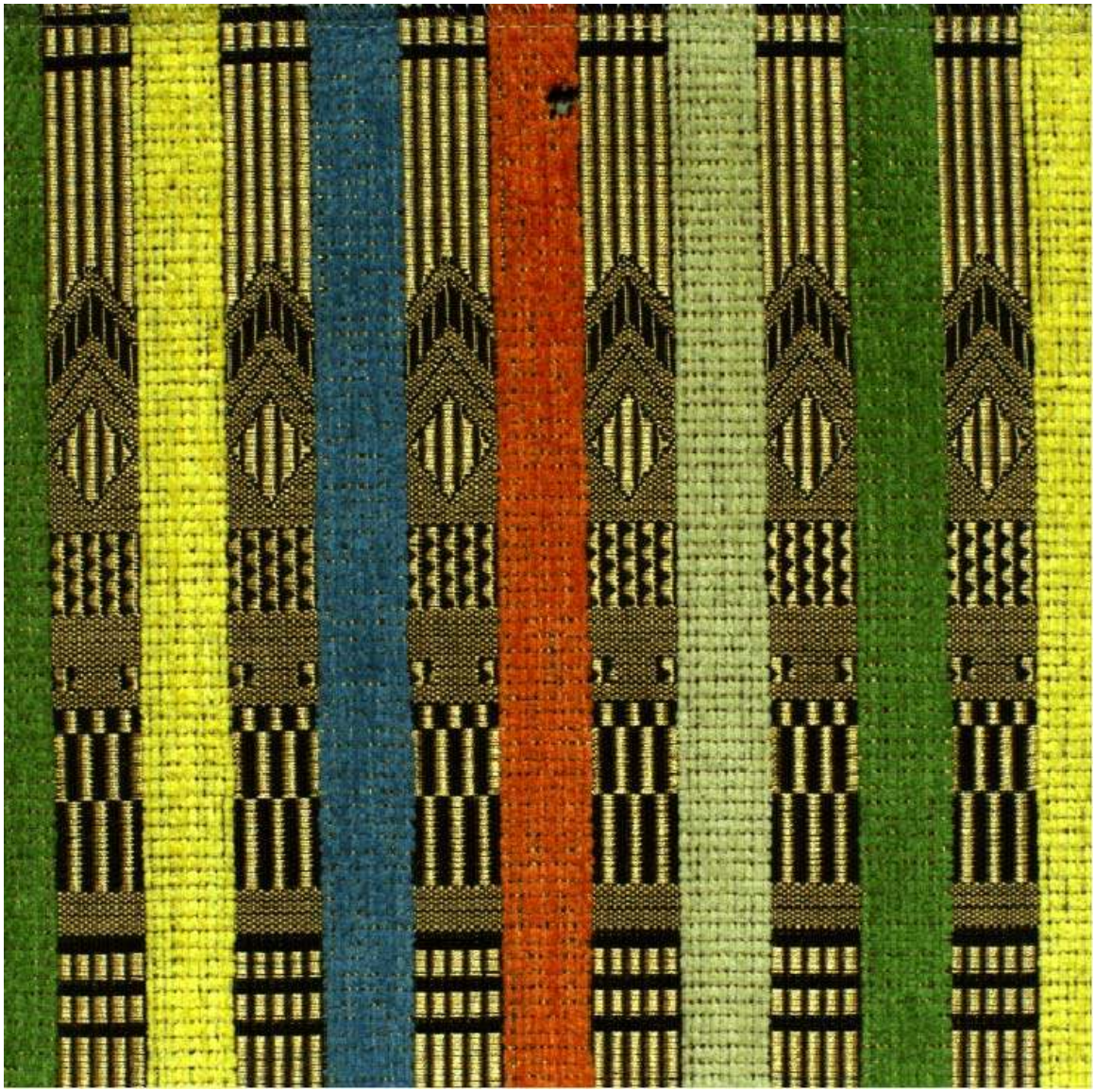

Figure 5 (a)

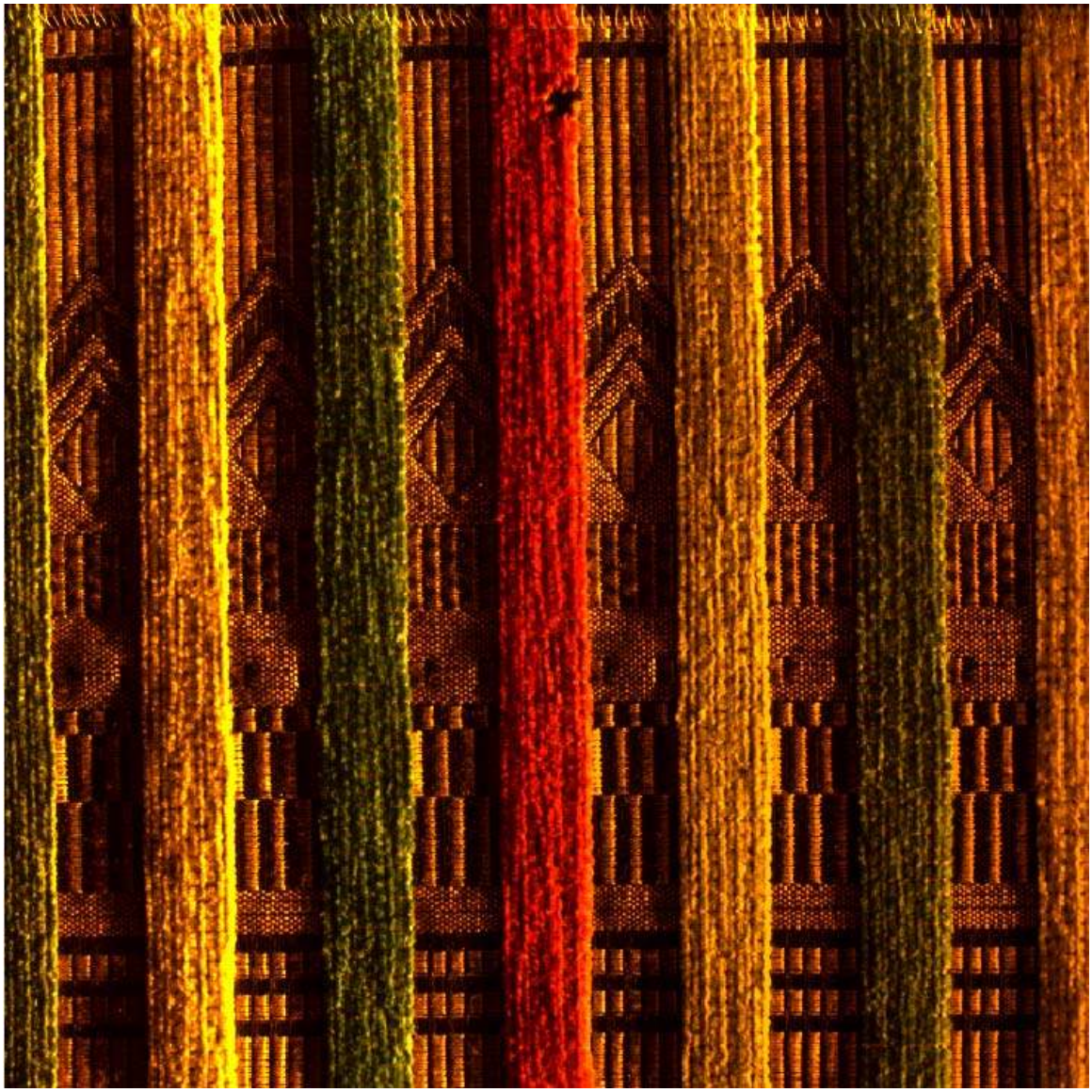

Figure 5 (b)

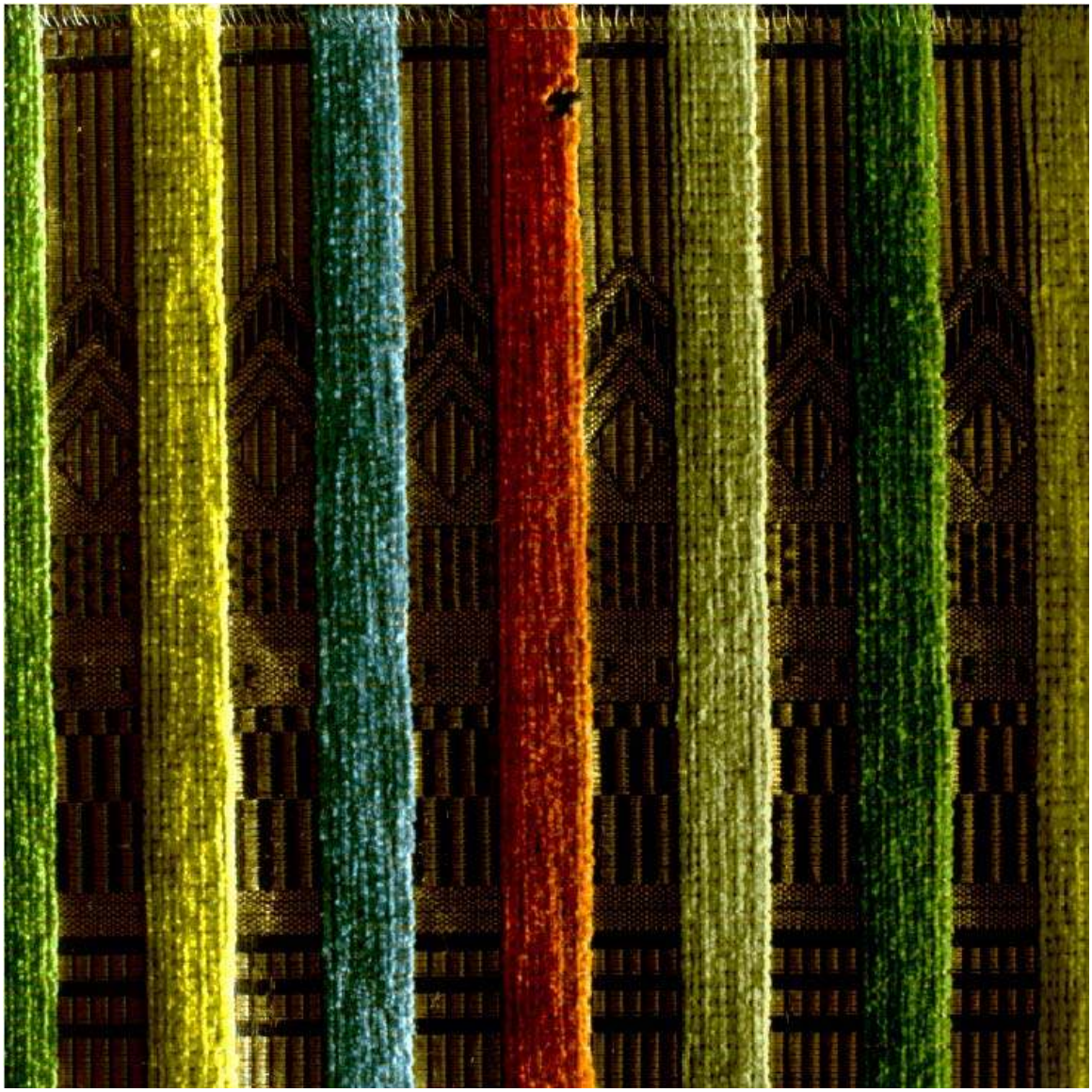

Figure 5 (c)

Figure 6 (a)

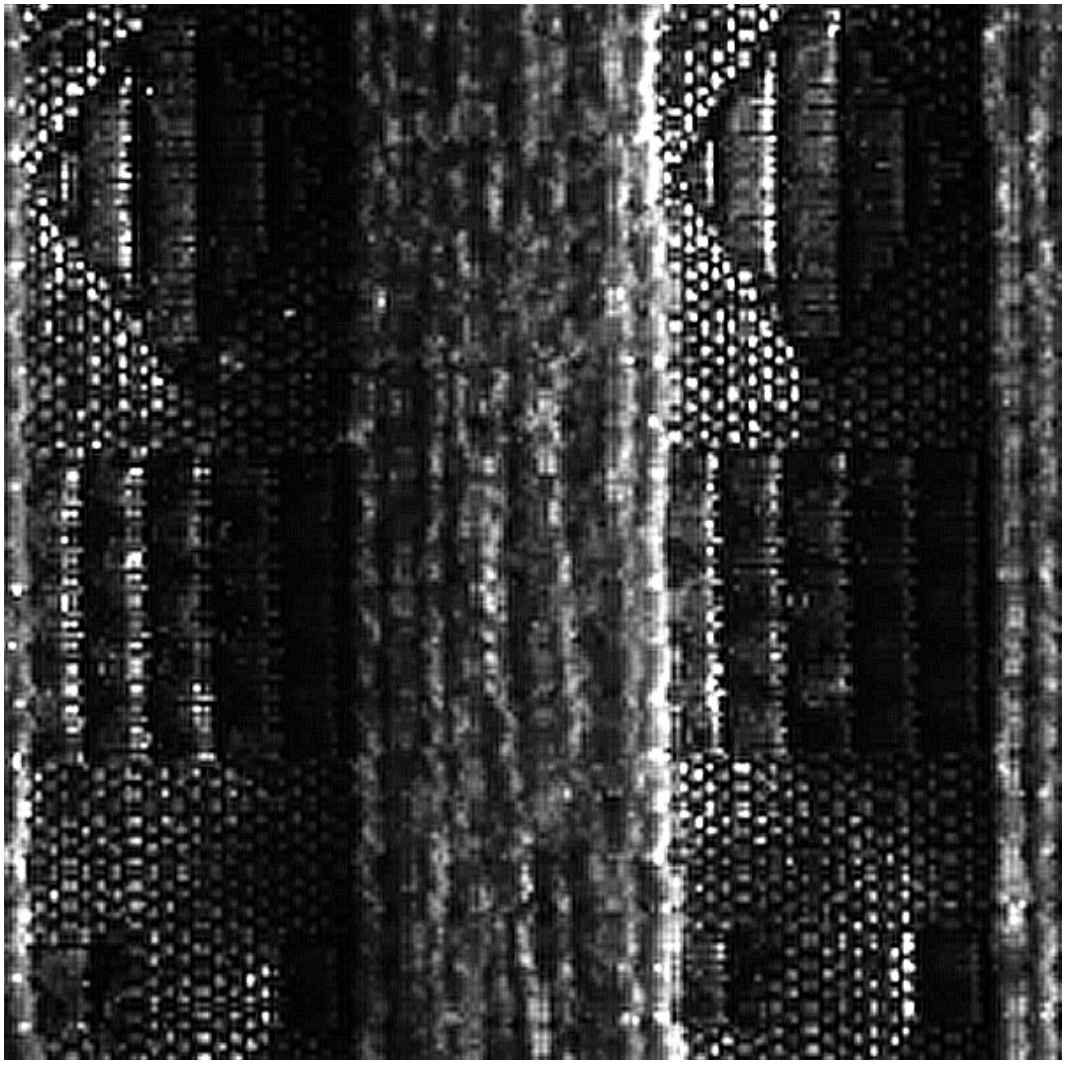

Figure 6 (b)

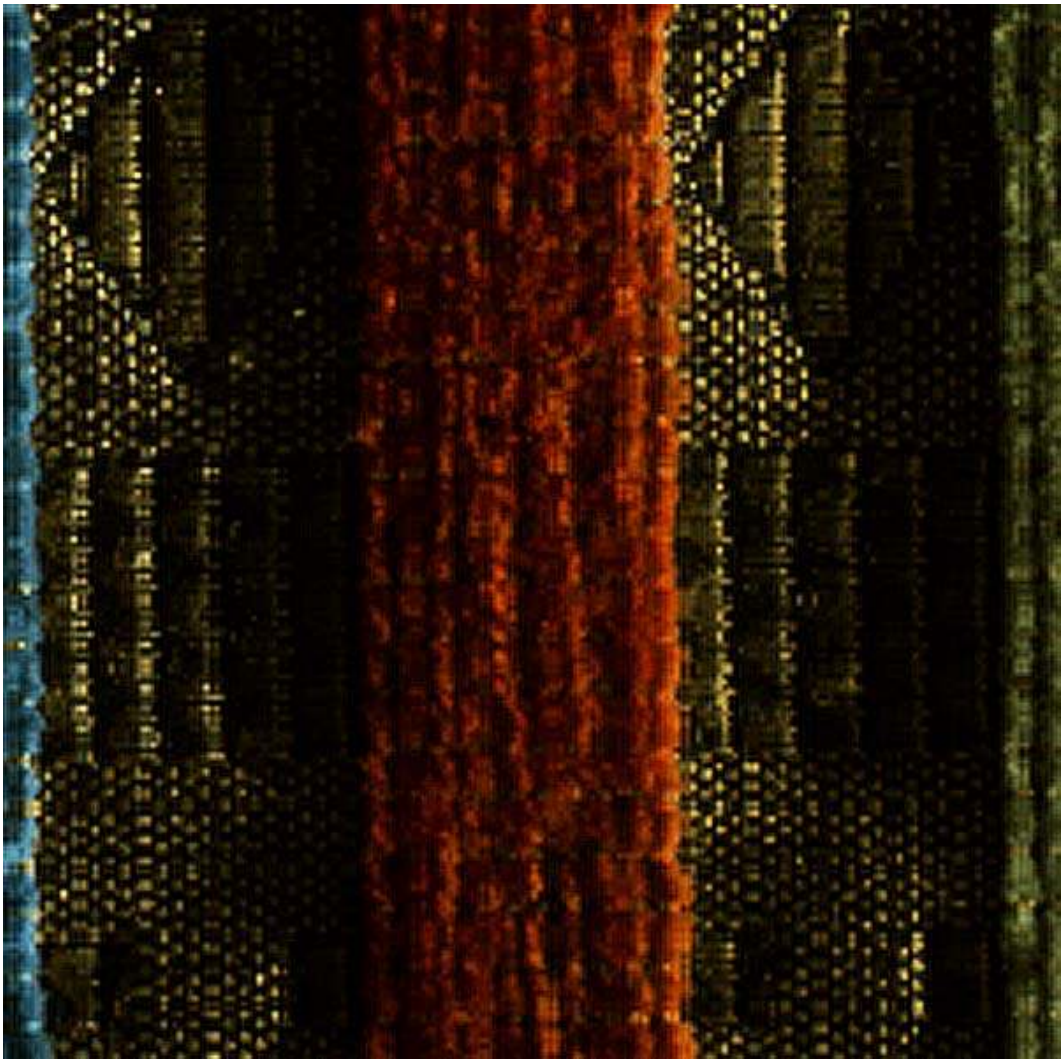

Figure 6 (c)